Theory of thermal conductivity of excitonic insulators

Shinta Takarada ,[1] Masao Ogata,[1,2] and Hiroyasu Matsuura[1]
[1]*Department of Physics, University of Tokyo, Bunkyo-ku, Tokyo 113-0033, Japan*
[2]*Trans-scale Quantum Science Institute, University of Tokyo, Bunkyo-ku, Tokyo 113-0033, Japan*

(Received 8 April 2021; revised 20 August 2021; accepted 27 September 2021; published 11 October 2021)

We study the thermal conductivity in an excitonic insulator using a simple quasi-one-dimensional two-band model consisting of electron and hole bands with the Coulomb interactions between these bands. Based on the linear response theory within a mean-field scheme, we develop a method to identify the contributions to thermal conductivity driven by the excitonic insulator. It is found that there is an additional heat current operator owing to the excitonic phase transition, and that it gives contributions to the thermal conductivity which are not expressed in the form of Sommerfeld-Bethe relations written in the form of an imaginary-time derivative of the electric current operator. Finally, we discuss the relationship between the additional contribution and the heat current carried by excitons.

DOI: 10.1103/PhysRevB.104.165122

I. INTRODUCTION

An excitonic insulator (EI) is one of the interesting correlated phases of narrow-gap semiconductors and semimetals. It was proposed in the 1960s that a Coulomb interaction between conduction band electrons and valence band holes can lead to a spontaneous formation of excitons, and their condensation induces a nonconducting state [1–6]. Various theoretical studies have been carried out on EI, and one of the most important and interesting aspects of these studies is that the excitonic theory can be transformed to the BCS theory by a particle-hole transformation [4–6]. Then, various properties such as anisotropic band structures [7], impurity effects [8], transport properties [5,9,10], and effects of a magnetic field [11] have been extensively discussed in terms of similarity or symmetry with the superconducting theory. However, materials identified as EI have yet to be defined.

Recently, a growing number of promising candidate materials for EI have actually been proposed, raising researchers' interest to study the EI phase. For example, Tm(Se, Te) [12,13], $1T$-$TiSe_2$ [14,15], and Ta_2NiSe_5 [16–18] have been proposed on the basis of various transport measurements [19,20], angle-resolved photoemission spectroscopy (ARPES) [15–17], and systematic elemental substitutions [21]. In particular, after Ta_2NiSe_5 was proposed, many experiments have been performed on Ta_2NiSe_5, such as spectroscopic ellipsometry [22], observation of electron-phonon coupling and exciton-phonon coupling [23–25], transport studies on bulk and thin-film samples [26], and the study of electrical tuning of the EI ground state [27]. The EI phase is also being actively studied theoretically, including calculations of the BCS-BEC crossover [28,29], electron-phonon coupling [30], spin-orbit coupling [31], the topological EI states [32], and the spin-triplet EI states in a two-dimensional system [33]. With that, the verification of theories and experiments has become increasingly important. It is interesting to note that some theoretical calculations reproduce the ARPES results [18], the superconductivity in the vicinity of the excitonic phase [34,35], and a peculiar temperature dependence of the orbital susceptibility [36,37].

Proposals of new candidate materials have also been pursued, such as semiconductor materials [38], graphene [39,40], and iron-based superconductors [41,42]. However, in actual materials, the EI phase often coexists with the charge density waves and staggered orbital orders [43,44], and it is still difficult to determine the EI state by experiments. Considering the verification of experimental and theoretical studies and the creation of new materials, it is important to develop methods other than photoemission spectroscopy to identify EI. Thermal conductivity in EI is also an interesting topic. This is because the excitons do not have electronic charges, but have energies contributing to the heat current. Indeed, it was observed that the thermal conductivity of $TmSe_{0.45}Te_{0.55}$, which is a candidate material of EI, shows an unusual temperature dependence [20].

When the thermal conductivity is written in the form of an imaginary-time derivative of the electric current, as shown by Jonson and Mahan [45], the following relations hold,

$$L_{11} = \int_{-\infty}^{\infty} d\epsilon \left(-\frac{d f(\epsilon)}{d\epsilon}\right)\sigma(\epsilon), \tag{1a}$$

$$L_{21} = \int_{-\infty}^{\infty} d\epsilon\, \frac{\epsilon-\mu}{e} \left(-\frac{d f(\epsilon)}{d\epsilon}\right)\sigma(\epsilon), \tag{1b}$$

$$L_{22} = \int_{-\infty}^{\infty} d\epsilon \left(\frac{\epsilon-\mu}{e}\right)^2 \left(-\frac{d f(\epsilon)}{d\epsilon}\right)\sigma(\epsilon), \tag{1c}$$

where the linear response coefficients, L_{ij} $(i, j = 1, 2)$, are defined by [46]

$$\boldsymbol{j} = L_{11}\boldsymbol{E} + L_{12}\left(-\frac{\nabla T}{T}\right),$$
$$\boldsymbol{j}^Q = L_{21}\boldsymbol{E} + L_{22}\left(-\frac{\nabla T}{T}\right). \tag{2}$$

Here, $\boldsymbol{j}$, $\boldsymbol{j}^Q$, $\boldsymbol{E}$, T, and ∇T are electric current density, heat current density, electric field, temperature, and temperature gradient, respectively, and e is the electron charge ($e < 0$) and $f(\epsilon) = 1/(e^{\beta(\epsilon-\mu)} + 1)$ is the Fermi distribution function, where $\beta = 1/k_B T$, and μ and k_B are the chemical potential and Boltzmann constant. Due to Onsager's reciprocal theorem, $L_{12} = L_{21}$ holds. The electrical conductivity is L_{11}, and the thermal conductivity κ, which is defined as the ratio of $\boldsymbol{j}_Q$ to $-\nabla T$ under the $\boldsymbol{j} = \boldsymbol{0}$ condition, is given by

$$\kappa = (L_{22} - L_{21}L_{12}/L_{11})/T. \tag{3}$$

Since excitons do not carry electrical charge, L_{11} in Eq. (1a) should be due to quasiparticles and not due to excitons. Correspondingly, L_{21} and L_{22} in Eqs. (1b) and (1c) should be also due to quasiparticles. Therefore, if the excitons, when they are condensed below the transition temperature, contribute to the heat current, then there must be additional contributions to L_{21} and L_{22} that are not expressed as in Eqs. (1b) and (1c). To clarify the discussion, in the following, we refer to Eqs. (1b) and (1c) as the Sommerfeld-Bethe (SB) relation for L_{21} [47] and SB relation for L_{22}, because Eqs. (1b) and (1c) can be obtained from the Boltzmann's equation [48]. In previous studies [10,49], the thermal conductivity was discussed on the basis of Eqs. (1a)–(1c). Thus, the exciton contributions were not taken into account.

In this paper, we study the thermal conductivity in a model for EI to identify the additional contribution derived from EI, which is beyond the SB relations. First, we microscopically obtain the heat current operator in a model for EI [37,50], or a simple quasi-one-dimensional two-band model. Then, we study the linear response theory [51,52] of L_{11}, L_{21}, and L_{22} within a mean-field scheme to introduce the order parameters of EI. We will show that, by considering two types of nearest-neighbor interactions, additional heat current operators owing to the EI phase transition exist and give the contributions in L_{21} and L_{22} which are not expressed in the form of Eqs. (1b) and (1c). Finally, we discuss the relationship between this additional contribution and the heat current due to excitons.

Theoretically, the validity of the SB relations, Eqs. (1a)–(1c), has been discussed [45,47,53]. Jonson and Mahan showed that, in the presence of a potential (including random potentials) and the electron-phonon interaction, the SB relations holds, except for a single term in the heat current operator which is due to the electron-phonon interaction [45]. Later, Kontani showed that the presence of the Hubbard interaction does not break the SB relations using the Jonson-Mahan method [53]. Recently, it has been shown that the presence of a finite range Coulomb interaction breaks the SB relations [47]. The present paper is an extension of Ref. [47] to the case where a phase transition occurs in the presence of finite range interactions.

This paper is organized as follows. In Sec. II, we introduce a model Hamiltonian to study the thermal conductivity in EI, and then develop a method for calculating the electronic state based on the mean-field approximation. In Sec. III, we derive heat current operators on this model microscopically. In Sec. IV, we clarify the contribution of the order parameters of EI to the thermal conductivity, and in Sec. V, we discuss the validity of SB relations on this model, and the relationship between the additional contribution and the heat current due to excitons. Finally, Sec. VI is devoted to the conclusion.

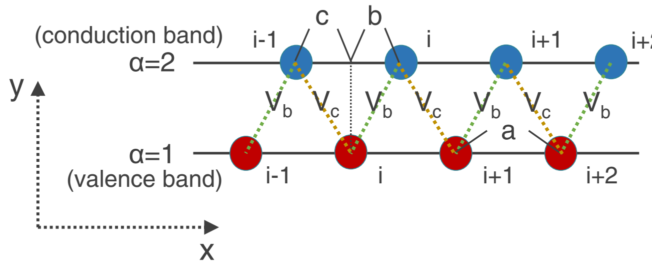

FIG. 1. Schematic picture of a two-band model with Coulomb interactions between the chains. Red and blue circles indicate the lattice sites, α is the index of the chain, b is the difference between the x coordinates of the ith site of two chains, and c is the difference between the ith and $(i-1)$th sites. V_b and V_c are the Coulomb interactions between the two chains.

II. TWO-BAND MODEL AND ELECTRONIC STATE OF AN EXCITONIC INSULATOR BASED ON THE MEAN-FIELD APPROXIMATION

To study EI, in this paper, we use the following two-band model Hamiltonian as shown in Fig. 1 [37],

$$\begin{aligned}\mathscr{H} = \sum_i [&(t\,\hat{c}^\dagger_{1,i}\,\hat{c}_{1,i+1} - t'\,\hat{c}^\dagger_{2,i}\,\hat{c}_{2,i+1} + \text{H.c.}) \\ &+ (-\epsilon-\mu)\hat{n}_{1,i} + (\epsilon-\mu)\hat{n}_{2,i} + V_b\,\hat{n}_{1,i}\,\hat{n}_{2,i} \\ &+ V_c\,\hat{n}_{1,i}\,\hat{n}_{2,i-1}] + \sum_{i,j,\alpha} V_{\text{imp}}(x_{\alpha,i} - X_j)\hat{n}_{\alpha,i},\end{aligned} \tag{4}$$

where t (t') and ϵ are a transfer integral between the nearest-neighbor sites in the chain $\alpha = 1$ ($\alpha = 2$), and a one-body level of the ith site, respectively. $\hat{c}_{\alpha,i}$ ($\hat{c}^\dagger_{\alpha,i}$) is an annihilation (creation) operator at the ith site of chain α where the spin degrees of freedom are neglected, and $\hat{n}_{\alpha,i} = \hat{c}^\dagger_{\alpha,i}\,\hat{c}_{\alpha,i}$. V_b and V_c indicate the Coulomb interaction between the ith site in the chain $\alpha = 1$ and the ith site in the chain $\alpha = 2$ and that between the ith site in the chain $\alpha = 1$ and the $(i-1)$th site in the chain $\alpha = 2$. Figure 1 shows the positions of sites. b (c) is the difference between the x coordinates of the ith site in the chain $\alpha = 1$ and the ith [$(i-1)$th] site in the chain $\alpha = 2$. We set the lattice constant a as $a = b + c$. $V_{\text{imp}}(x_{\alpha,i} - X_j)$ is the randomly distributed impurity potential where $x_{\alpha,i}$ and X_j are the x coordinates of the position of the site and randomly distributed impurities, respectively. In this paper, we consider the effects of impurities in two ways. One is impurity scattering which leads to the relaxation rate of electrons and holes. The other is the impurity contribution to the heat current. These effects will be discussed in Secs. III and IV. So we neglect V_{imp} in this section.

A similar effective model has been suggested in Ref. [37]. The model of Ref. [37] corresponds to that for $c = a$, $b = 0$, and $V_c = 0$ in Eq. (4). As discussed below, finite b and V_c are important to obtain the additional heat current due to the Coulomb interaction, which breaks the SB relations.

Using a mean-field approximation for EI and assuming that the order parameters are independent of the sites, i.e.,

$$\Delta_b = -\frac{V_b}{N}\sum_i \langle \hat{c}^\dagger_{2,i}\,\hat{c}_{1,i}\rangle = -\frac{V_b}{N}\sum_k \langle \hat{c}^\dagger_{2,k}\,\hat{c}_{1,k}\rangle e^{-ikb},$$
$$\Delta_c = -\frac{V_c}{N}\sum_i \langle \hat{c}^\dagger_{2,i-1}\,\hat{c}_{1,i}\rangle = -\frac{V_c}{N}\sum_k \langle \hat{c}^\dagger_{2,k}\,\hat{c}_{1,k}\rangle e^{ikc}, \quad (5)$$

with N being the total number of sites, we obtain the following mean-field Hamiltonian of EI,

$$\begin{aligned}\mathscr{H}_{\rm MF} = &\sum_k \{(2t\cos ka - \epsilon - \mu)\hat{c}^\dagger_{1,k}\,\hat{c}_{1,k}\\ &+ (-2t'\cos ka + \epsilon - \mu)\hat{c}^\dagger_{2,k}\,\hat{c}_{2,k}\\ &+ (\,\Delta_k\,\hat{c}^\dagger_{1,k}\,\hat{c}_{2,k} + \text{H.c.})\}\\ &+ \sum_{k,q,\alpha}\frac{1}{N}\,\rho_{\rm imp}(q)v_{\rm imp}(q)\hat{c}^\dagger_{\alpha,k+q}\,\hat{c}_{\alpha,k},\end{aligned} \quad (6)$$

where $\Delta_k \equiv \Delta_b\,e^{ikb} + \Delta_c\,e^{-ikc}$, $\rho_{\rm imp}(q) \equiv \sum_j e^{-iqX_j}$, and $v_{\rm imp}(q) \equiv \sum_i e^{-iq(x_{\alpha,i}-X_j)}\,V_{\rm imp}(x_{\alpha,i} - X_j)$ $\approx \frac{1}{a}\int dx\,e^{-iqx}V_{\rm imp}(x)$. Note that the mean-field approximation of $\langle \hat{c}^\dagger_1\,\hat{c}_1\rangle$ form can be ignored because it merely gives a change in the on-site energy, which will not be important for discussing EI.

By diagonalizing this Hamiltonian except for the impurity potential, we obtain

$$\mathscr{H}_{\rm eff} = \sum_k (E_{k+}\,\hat{p}^\dagger_{k+}\,\hat{p}_{k+} + E_{k-}\,\hat{p}^\dagger_{k-}\,\hat{p}_{k-}), \quad (7)$$

where $\hat{p}_{k\pm}$ is an annihilation operator of a quasiparticle, and the quasiparticle energy is given by

$$\begin{aligned}E_{k\pm} =& (t - t')\cos ka - \mu\\ &\pm \sqrt{\{(t + t')\cos ka - \epsilon\}^2 + |\Delta_k|^2}.\end{aligned} \quad (8)$$

The unitary matrix satisfying $\binom{\hat{c}_{1,k}}{\hat{c}_{2,k}} \equiv \boldsymbol{U}\binom{\hat{p}_{k+}}{\hat{p}_{k-}}$ is

$$\boldsymbol{U} = \frac{1}{\sqrt{2X_k}}\begin{pmatrix}\frac{\Delta_k}{\sqrt{X_k - Y_k}} & \frac{\Delta_k}{\sqrt{X_k + Y_k}}\\ \frac{X_k - Y_k}{\sqrt{X_k - Y_k}} & \frac{-X_k - Y_k}{\sqrt{X_k + Y_k}}\end{pmatrix}, \quad (9)$$

where X_k and Y_k are

$$\begin{aligned}X_k &\equiv \sqrt{\{(t + t')\cos ka - \epsilon\}^2 + |\Delta_k|^2},\\ Y_k &\equiv (t + t')\cos ka - \epsilon.\end{aligned} \quad (10)$$

Using the effective Hamiltonian of Eq. (7), the self-consistent equations to obtain the order parameters of EI become

$$\Delta_b = -\frac{V_b}{2N}\sum_k (\Delta_b + \Delta_c\,e^{-ika})\frac{f(E_{k+}) - f(E_{k-})}{X_k},$$
$$\Delta_c = -\frac{V_c}{2N}\sum_k (\Delta_b\,e^{ika} + \Delta_c)\frac{f(E_{k+}) - f(E_{k-})}{X_k}. \quad (11)$$

The chemical potential is now included in $E_{k\pm}$. Since we focus on the half-filling case in this paper, the chemical potential is

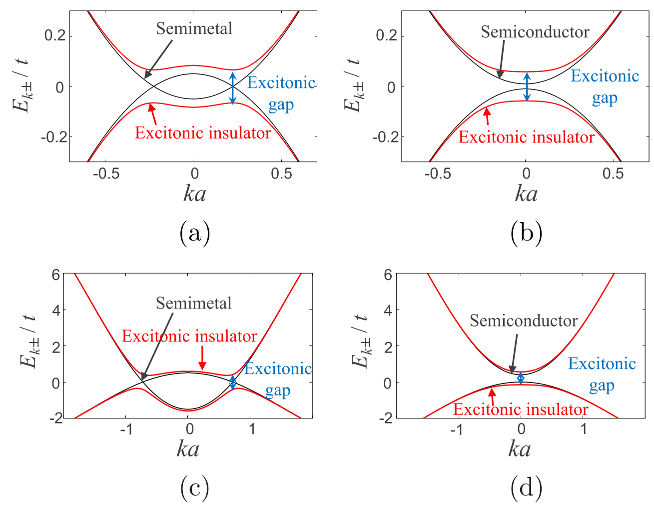

FIG. 2. Dispersion relations of the normal state (black line) and EI (red line) at $T/t = 0$. The parameters are set as (a) $t' = t$, $V_b = V_c = 0.5t$, and $\epsilon = 1.95t$, (b) $t' = t$, $V_b = V_c = 0.5t$, and $\epsilon = 2.01t$, (c) $t' = 3t$, $V_b = V_c = 2t$, and $\epsilon = 3t$, and (d) $t' = 3t$, $V_b = V_c = 2t$, and $\epsilon = 4.2t$.

determined by

$$\frac{1}{N}\sum_k \{f(E_{k+}) + f(E_{k-})\} = 1. \quad (12)$$

Solving Eqs. (11) and (12) self-consistently, we can obtain Δ_b, Δ_c, and μ. It is to be noted that the order parameters can be complex. However, we find that the phase difference between Δ_b and Δ_c does not occur in the parameters we used in this paper. Thus, we set the order parameters as real numbers.

Figure 2 shows the dispersion relations of normal state (black lines) and EI (red lines) at $T/t = 0$ for several values of Hamiltonian parameters. We set $t' = t$, $V_b = V_c = 0.5t$, and $\epsilon = 1.95t$ for Fig. 2(a) and $\epsilon = 2.01t$ for Fig. 2(b), and $t' = 3t$, $V_b = V_c = 2t$, and $\epsilon = 3t$ for Fig. 2(c) and $\epsilon = 4.2t$ for Fig. 2(d), respectively. Figures 2(a) and 2(b) are examples of the case with particle-hole symmetry, and Figs. 2(c) and 2(d) are examples of the case without it. The dispersion relations of the normal state indicate the semimetallic state for Figs. 2(a) and 2(c), or the semiconducting state for Figs. 2(b) and 2(d). When we consider the order parameters of EI, all the electronic states become semiconducting states.

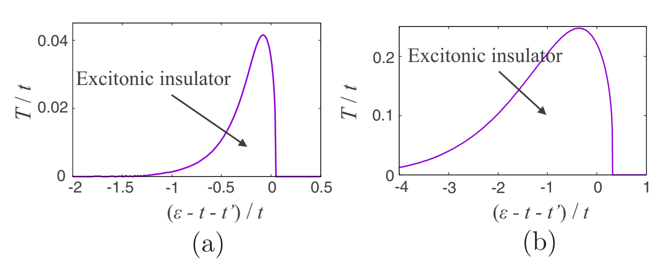

FIG. 3. ϵ dependence of the transition temperature at (a) $t' = t$ and $V_b = V_c = 0.5t$ and (b) $t' = 3t$ and $V_b = V_c = 2t$.

Figures 3(a) and 3(b) show the ϵ dependence of the transition temperature of EI. The parameters of Fig. 3(a) [Fig. 3(b)] are the same as that of Fig. 2(a) [Fig. 2(c)]. As shown in Figs. 3(a) and 3(b), the transition temperature has a maximum at $(\epsilon - t - t')/t \sim 0$. This ϵ behavior is the same as the result of Ref. [37].

III. ELECTRIC AND HEAT CURRENT OPERATORS

The electric current density operator $\hat{\boldsymbol{j}}(\boldsymbol{r})$ and the heat current density operator $\hat{\boldsymbol{j}}^Q(\boldsymbol{r})$ are derived from the continuity equations [46]

$$\frac{d\hat{\rho}(\boldsymbol{r})}{dt} + \mathrm{div}\,\hat{\boldsymbol{j}}(\boldsymbol{r}) = 0, \qquad \frac{d\hat{h}(\boldsymbol{r})}{dt} + \mathrm{div}\,\hat{\boldsymbol{j}}^Q(\boldsymbol{r}) = 0, \tag{13}$$

where $\hat{\rho}(\boldsymbol{r})$ and $\hat{h}(\boldsymbol{r})$ are the charge density and the Hamiltonian density [$\mathscr{H} = \int d\boldsymbol{r}\,\hat{h}(\boldsymbol{r})$], respectively.

In the preset model [Eq. (4)], the total electric current operator, $\hat{J} = \int d\boldsymbol{r}\,\hat{j}(\boldsymbol{r})$, is given by

$$\hat{J} = \sum_{k,\alpha} j_\alpha(k)\hat{c}^\dagger_{\alpha,k}\,\hat{c}_{\alpha,k}, \tag{14}$$

with

$$j_1(k) \equiv -\frac{2ea}{\hbar}t\sin ka, \qquad j_2(k) \equiv \frac{2ea}{\hbar}t'\sin ka. \tag{15}$$

On the other hand, the total heat current operator, $\hat{J}^Q = \int d\boldsymbol{r}\,\hat{j}^Q(\boldsymbol{r})$, becomes

$$\hat{J}^Q = \sum_{k,\alpha} j^Q_{\alpha\alpha}(k)\hat{c}^\dagger_{\alpha,k}\,\hat{c}_{\alpha,k} + \sum_{k,k',q} j^Q_V(k,k',q)\hat{c}^\dagger_{1,k+q}\,\hat{c}_{1,k}\,\hat{c}^\dagger_{2,k'-q}\,\hat{c}_{2,k'} + \sum_{k,q,\alpha} j^Q_{\mathrm{imp}\alpha}(k,q)\hat{c}^\dagger_{\alpha,k+q}\,\hat{c}_{\alpha,k}, \tag{16}$$

with

$$\begin{aligned}
j^Q_{11}(k) &\equiv -\frac{2a}{\hbar}t\sin ka(2t\cos ka - \epsilon - \mu),\\
j^Q_{22}(k) &\equiv \frac{2a}{\hbar}t'\sin ka(-2t'\cos ka + \epsilon - \mu),\\
j^Q_V(k,k',q) &\equiv -\frac{a}{\hbar}(t-t')\frac{1}{N}\left\{(V_b e^{iqb} + V_c e^{-iqc})\cos\frac{q}{2}a\sin\left(k+\frac{q}{2}\right)a + \left(V_b e^{iq(b+\frac{a}{2})} + V_c e^{-iq(c+\frac{a}{2})}\right)\sin\left(k'-\frac{q}{2}\right)a\right\},\\
j^Q_{\mathrm{imp}1}(k,q) &\equiv -\frac{2a}{\hbar}t\frac{1}{N}\rho_{\mathrm{imp}}(q)v_{\mathrm{imp}}(q)\cos\frac{q}{2}a\sin\left(k+\frac{q}{2}\right)a,\\
j^Q_{\mathrm{imp}2}(k,q) &\equiv \frac{2a}{\hbar}t'\frac{1}{N}\rho_{\mathrm{imp}}(q)v_{\mathrm{imp}}(q)\cos\frac{q}{2}a\sin\left(k+\frac{q}{2}\right)a.
\end{aligned} \tag{17}$$

The derivations of these operators together with the Hamiltonian density are shown in Appendix A. While $\hat{J}$ in Eq. (14) is a one-body current operator, the heat current operator $\hat{J}^Q$ in Eq. (16) is the many-body operator in the presence of the Coulomb interaction [47].

As discussed in Appendix B, if we start from the mean-field Hamiltonian of Eq. (6), we obtain a different expression for the heat current operator. However, the heat current operator in Eq. (16) should be used to study the thermal conductivity, because it satisfies the continuity equation (13) without any approximations.

IV. ADDITIONAL HEAT CURRENT CONTRIBUTION IN THE EI PHASE

In this section, we study thermal conductivity based on the linear response theory within the mean-field approximation to clarify the additional contributions in the EI phase, which do not satisfy the SB relation in Eqs. (1).

In the mean-field approximation (6), the one-body Green's function is given as

$$\mathscr{G}^0_{\alpha\alpha'}(k,\tau) \equiv -\langle T_\tau[\,\hat{p}_{k\alpha}(\tau)\hat{p}^\dagger_{k\alpha'}(0)]\rangle, \tag{18}$$

$$\begin{aligned}
\boldsymbol{G}^{(0)}(k,i\epsilon_n) &\equiv \begin{pmatrix} \mathscr{G}^0_{++}(k,i\epsilon_n) & \mathscr{G}^0_{+-}(k,i\epsilon_n)\\ \mathscr{G}^0_{-+}(k,i\epsilon_n) & \mathscr{G}^0_{--}(k,i\epsilon_n)\end{pmatrix}\\
&= \begin{pmatrix} \frac{1}{i\epsilon_n - E_{k+}} & 0\\ 0 & \frac{1}{i\epsilon_n - E_{k-}}\end{pmatrix},
\end{aligned} \tag{19}$$

where T_τ is the standard τ-ordering operator, and $\epsilon_n = (2n+1)\pi k_B T$ where n is an integer. Taking into account the self-energy due to the impurity scattering

$$\boldsymbol{\Sigma}(k,i\epsilon_n) = -\,i\,\mathrm{sgn}(\epsilon_n)\begin{pmatrix}\Gamma_1 & \Gamma_3\\ \Gamma_3 & \Gamma_2\end{pmatrix}, \tag{20}$$

where Γ_1, Γ_2, and Γ_3 are real, independent of ϵ_n, Dyson's equation leads to

$$\boldsymbol{G}(k,i\epsilon_n) = \frac{1}{[i\epsilon_n - E_{k+} + i\,\mathrm{sgn}(\epsilon_n)\Gamma_1][i\epsilon_n - E_{k-} + i\,\mathrm{sgn}(\epsilon_n)\Gamma_2] + \Gamma_3^2}\begin{pmatrix} i\epsilon_n - E_{k-} + i\,\mathrm{sgn}(\epsilon_n)\Gamma_2 & -i\,\mathrm{sgn}(\epsilon_n)\Gamma_3\\ -i\,\mathrm{sgn}(\epsilon_n)\Gamma_3 & i\epsilon_n - E_{k+} + i\,\mathrm{sgn}(\omega_n)\Gamma_1\end{pmatrix}. \tag{21}$$

In this paper, the values of Γ_1, Γ_2, and Γ_3 are estimated by calculating the self-energy in the absence of interactions from Dyson's equation as follows,

$$\begin{aligned}\Gamma_1 &= \frac{an_i v^2}{2X_k}\left(\frac{X_k+Y_k}{\sqrt{4t^2-(\epsilon+\mu)^2}}+\frac{X_k-Y_k}{\sqrt{4t'^2-(\epsilon-\mu)^2}}\right),\\ \Gamma_2 &= \frac{an_i v^2}{2X_k}\left(\frac{X_k-Y_k}{\sqrt{4t^2-(\epsilon+\mu)^2}}+\frac{X_k+Y_k}{\sqrt{4t'^2-(\epsilon-\mu)^2}}\right),\\ \Gamma_3 &= \frac{an_i v^2}{2X_k}\left(\frac{|\Delta_k|}{\sqrt{4t^2-(\epsilon+\mu)^2}}+\frac{|\Delta_k|}{\sqrt{4t'^2-(\epsilon-\mu)^2}}\right).\end{aligned} \tag{22}$$

Here, n_i is the impurity density. For simplicity, we assume that $V_{\rm imp}(x_{\alpha,i}-X_j)$ in Eq. (4) has the form of a delta function. In this case, $v_{\rm imp}(q)$ is independent of q, and we put $v_{\rm imp}(q)=v$.

We also apply the mean-field approximation to the heat current operator to obtain

$$\begin{aligned}\hat{J}^Q_{\rm MF} = &\sum_{k,\alpha,\alpha'} j^Q_{\alpha\alpha'}(k)\hat{c}^\dagger_{\alpha,k}\hat{c}_{\alpha',k}\\ &+\sum_{k,q,\alpha} j^Q_{{\rm imp}\alpha}(k,q)\hat{c}^\dagger_{\alpha,k+q}\hat{c}_{\alpha,k},\end{aligned} \tag{23}$$

where j^Q_{12} and j^Q_{21} are

$$\begin{aligned}j^Q_{12}(k) &= \overline{j^Q_{21}(k)}\\ &\equiv -\frac{a}{\hbar}(t-t')\Bigg\{\Delta_k\sin ka\\ &\quad+\frac{i}{4}\left(\frac{V_c}{V_b}\Delta_b e^{-ikc}-\frac{V_b}{V_c}\Delta_c e^{ikb}\right)\\ &\quad-\frac{i}{2}(\Delta_b e^{ikb}-\Delta_c e^{-ikc})\cos ka\Bigg\}.\end{aligned} \tag{24}$$

We will proceed with the calculation assuming that the effect of impurities is sufficiently small. From Eq. (17), it can be seen that the heat current $j^Q_{\rm imp1}(k,q)$ and $j^Q_{\rm imp2}(k,q)$ due to impurities only have effects of the order of $O(v_{\rm imp})$ or $O(v^2_{\rm imp})$, which is smaller than the other heat current. Therefore, the heat current due to impurities will be ignored in the following calculations. We also ignore the vertex correction due to impurities as well, since it only affects the current and heat current operators of the order of $O(v^2_{\rm imp})$.

Using the annihilation and creation operators of a quasiparticle, $\hat{p}^\dagger_{k\alpha}$ and $\hat{p}_{k\alpha}$, the electric current and heat current operators are written as

$$\begin{aligned}\hat{J} &= \sum_k(\hat{p}^\dagger_{k+}\quad\hat{p}^\dagger_{k-})\boldsymbol{\Gamma}(k)\begin{pmatrix}\hat{p}_{k+}\\ \hat{p}_{k-}\end{pmatrix},\\ \hat{J}^Q_{\rm MF} &= \sum_k(\hat{p}^\dagger_{k+}\quad\hat{p}^\dagger_{k-})\boldsymbol{\Gamma}^Q(k)\begin{pmatrix}\hat{p}_{k+}\\ \hat{p}_{k-}\end{pmatrix},\end{aligned} \tag{25}$$

where $\boldsymbol{\Gamma}=\boldsymbol{U}^\dagger\begin{pmatrix} j_1 & 0\\ 0 & j_2\end{pmatrix}\boldsymbol{U}$, $\boldsymbol{\Gamma}^Q=\boldsymbol{U}^\dagger\begin{pmatrix} j^Q_{11} & j^Q_{12}\\ j^Q_{21} & j^Q_{22}\end{pmatrix}\boldsymbol{U}$.

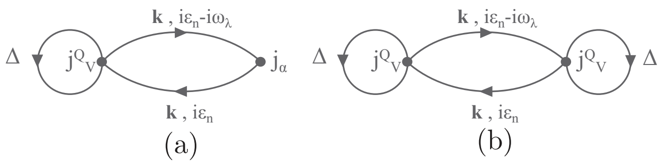

FIG. 4. Feynman diagrams for heat currents including interactions.

L_{11} is obtained by the $\hat{J}$-$\hat{J}$ correlation

$$\begin{aligned}\Phi_{11}(\tau) &= \frac{1}{aN}\langle T_\tau[\hat{J}(\tau)\hat{J}(0)]\rangle\\ &= -\frac{1}{aN}\sum_k {\rm Tr}[\boldsymbol{\Gamma}(k)\boldsymbol{G}(k,\tau)\boldsymbol{\Gamma}(k)\boldsymbol{G}(k,-\tau)],\end{aligned} \tag{26}$$

and its Fourier transform

$$\begin{aligned}\Phi_{11}(i\omega_\lambda) = -\frac{k_BT}{aN}\sum_k\sum_n {\rm Tr}[&\boldsymbol{\Gamma}(k)\boldsymbol{G}(k,i\epsilon_n)\\ &\times\boldsymbol{\Gamma}(k)\boldsymbol{G}(k,i\epsilon_n-i\omega_\lambda)].\end{aligned} \tag{27}$$

Here, $\omega_\lambda=2\lambda\pi k_BT$ and λ is an integer.

By performing the analytic continuation ($i\omega_\lambda\to\hbar\omega+i\delta$), we can obtain

$$L_{11}=\lim_{\omega\to0}\frac{\Phi_{11}(\hbar\omega+i\delta)-\Phi_{11}(0)}{i\omega}. \tag{28}$$

Similarly, L_{21}, L_{22} can be calculated by

$$\begin{aligned}\Phi_{21}(i\omega_\lambda) = -\frac{k_BT}{aN}\sum_k\sum_n {\rm Tr}[&\boldsymbol{\Gamma}^Q(k)\boldsymbol{G}(k,i\epsilon_n)\\ &\times\boldsymbol{\Gamma}(k)\boldsymbol{G}(k,i\epsilon_n-i\omega_\lambda)],\end{aligned} \tag{29}$$

$$\begin{aligned}\Phi_{22}(i\omega_\lambda) = -\frac{k_BT}{aN}\sum_k\sum_n {\rm Tr}[&\boldsymbol{\Gamma}^Q(k)\boldsymbol{G}(k,i\epsilon_n)\\ &\times\boldsymbol{\Gamma}^Q(k)\boldsymbol{G}(k,i\epsilon_n-i\omega_\lambda)].\end{aligned} \tag{30}$$

Equations (29) and (30) correspond to the Feynman diagrams shown in Fig. 4.

We can see that the dominant contributions are in the order of $O(1/\Gamma_1)$, $O(1/\Gamma_2)$ and $O(1/\Gamma_3)$. Then, ignoring the higher order of $O(\Gamma_1)$, $O(\Gamma_2)$, and $O(\Gamma_3)$, we obtain the correlation functions as follows,

$$L_{11}=\int d\epsilon\left(-\frac{df(\epsilon)}{d\epsilon}\right)\sigma(\epsilon), \tag{31a}$$

$$L_{21}=\int d\epsilon\,\frac{\epsilon-\mu}{e}\left(-\frac{df(\epsilon)}{d\epsilon}\right)[\sigma(\epsilon)+\sigma_1(\epsilon)], \tag{31b}$$

$$L_{22}=\int d\epsilon\left(\frac{\epsilon-\mu}{e}\right)^2\left(-\frac{df(\epsilon)}{d\epsilon}\right)[\sigma(\epsilon)+2\sigma_1(\epsilon)+\sigma_2(\epsilon)], \tag{31c}$$

where $\sigma(\epsilon)$, $\sigma_1(\epsilon)$, and $\sigma_2(\epsilon)$ are

$$\begin{aligned}\sigma(\epsilon)\equiv\frac{e^2a^2}{4\pi\hbar}\int dk\Bigg\{&\delta(\epsilon-\mu-E_{k+})\frac{\sigma^2_{k+}}{\Gamma_1}\\ &+\delta(\epsilon-\mu-E_{k-})\frac{\sigma^2_{k-}}{\Gamma_2}\Bigg\},\end{aligned} \tag{32}$$

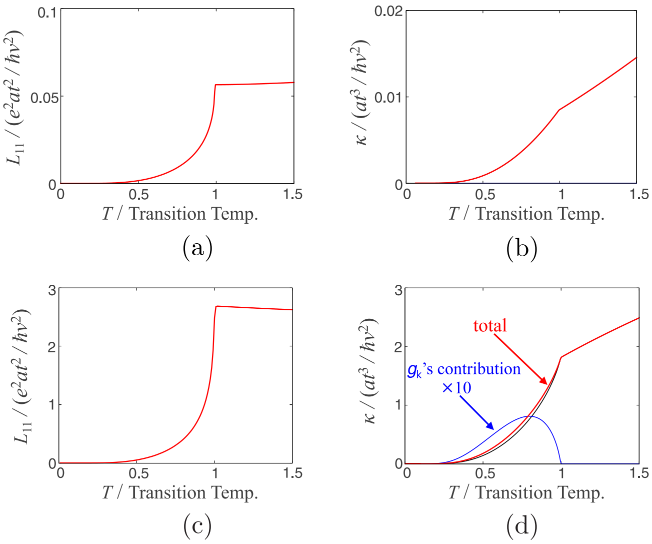

FIG. 5. Temperature dependence on (a) L_{11} and (b) κ at $t' = t$, $V_b = V_c = 0.5t$, $\epsilon = 1.95t$, and (c) L_{11} and (d) κ at $t' = 3t$, $V_b = V_c = 2t$, $\epsilon = 3t$. Blue, black, and red lines indicate the contribution from $g_k \times 10$, other terms, and total, respectively.

$$\sigma_1(\epsilon) \equiv \frac{e^2a^2}{4\pi\hbar}\int dk\left\{\delta(\epsilon-\mu-E_{k+})\frac{g_k\sigma_{k+}}{E_{k+}\Gamma_1} - \delta(\epsilon-\mu-E_{k-})\frac{g_k\sigma_{k-}}{E_{k-}\Gamma_2}\right\}, \tag{33}$$

$$\sigma_2(\epsilon) \equiv \frac{e^2a^2}{4\pi\hbar}\int dk\left\{\delta(\epsilon-\mu-E_{k+})\frac{g_k^2}{E_{k+}^2\Gamma_1} + \delta(\epsilon-\mu-E_{k-})\frac{g_k^2}{E_{k-}^2\Gamma_2}\right\}, \tag{34}$$

$$\sigma_{k\pm} \equiv \frac{\sin ka}{X_k}\{(X_k \pm Y_k)t - (X_k \mp Y_k)t'\}, \tag{35}$$

$$g_k \equiv \frac{t-t'}{4X_k}\left\{\left(\frac{V_c}{V_b}\Delta_b^2 + \frac{V_b}{V_c}\Delta_c^2\right)\sin ka + 2\Delta_b\Delta_c\sin 2ka\right\}. \tag{36}$$

Derivations of Eqs. (31) are given in Appendix C.

L_{21} and L_{22} differ from L_{11} in that g_k appears in the integrand when $t \neq t'$. In other words, since $\sigma(\epsilon)$ is contained in all of L_{11}, L_{21}, and L_{22}, the first terms in L_{21} and L_{22} are expressed by the SB relations. However, the second term in L_{21} and the second and third terms in L_{22} are not expressed by the SB relations because $\sigma_1(\epsilon)$ and $\sigma_2(\epsilon)$ are not included in L_{11}. Therefore, these terms give the additional contributions to the thermal conductivity in the EI phase. This is the main result of this paper, and we will discuss it in more detail in the next section.

Before going into details, let us see the magnitude of these additional contributions. Figures 5(a) and 5(b) [Figs. 5(c) and 5(d)] show the temperature dependence of L_{11} and κ at $t' = t$, $V_b = V_c = 0.5t$, and $\epsilon = 1.95t$ (at $t' = 3t$, $V_b = V_c = 2t$, and $\epsilon = 3t$). The portion of κ that is related to g_k is indicated by the blue line, the others by the black line, and the total by the red line.

It is found that the contribution of g_k to the thermal conductivity is present below the transition temperature. When $t = t'$, the thermal conductivity follows the SB relation because $g_k = 0$ [Fig. 5(b)], but when $t \neq t'$, it may be visible depending on the parameters [Fig. 5(d)]. This is the thermal conductivity produced by the additional heat current driven by EI.

V. DISCUSSIONS

As mentioned in Sec. I, when the heat current operator $\widetilde{\hat{J}^Q}(\tau)$ can be written in the form of an imaginary-time derivative of the electric current $[\hat{J}(\tau,\tau') = \sum_k\{j(k)\hat{c}_k^\dagger(\tau)\hat{c}_k(\tau')\}]$ as

$$\widetilde{\hat{J}^Q}(\tau) = \lim_{\tau'\to\tau}\frac{1}{2}\left(\frac{\partial}{\partial\tau} - \frac{\partial}{\partial\tau'}\right)\hat{J}(\tau,\tau'), \tag{37}$$

L_{11}, L_{21}, and L_{22} are expressed by Eqs. (1) [45,47], where $\hat{c}_k(\tau)$ is an annihilation operator with an imaginary-time dependence.

In the present case of a mean-field approximation, if we consider that the imaginary-time derivatives of τ and τ' are given by the mean-field Hamiltonian (6) as

$$\frac{\partial}{\partial\tau}\hat{J}(\tau,\tau') = \sum_k j(k)[\hat{\mathscr{H}}_{\rm MF}(\tau), \hat{c}_k^\dagger(\tau)]\hat{c}_k(\tau'),$$
$$\frac{\partial}{\partial\tau'}\hat{J}(\tau,\tau') = \sum_k j(k)\hat{c}_k^\dagger(\tau)[\hat{\mathscr{H}}_{\rm MF}(\tau'), \hat{c}_k(\tau')], \tag{38}$$

we obtain

$$\begin{aligned}\widetilde{\hat{J}^Q}(\tau) &= \lim_{\tau'\to\tau}\frac{1}{2}\left(\frac{\partial}{\partial\tau} - \frac{\partial}{\partial\tau'}\right)\hat{J}(\tau,\tau') \\ &= \sum_{k,\alpha,\alpha'} j'^Q_{\alpha\alpha'}(k)\hat{c}_{\alpha,k}^\dagger(\tau)\hat{c}_{\alpha',k}(\tau) \\ &\quad + \sum_{k,q,\alpha} j^Q_{{\rm imp}\alpha}(k,q)\hat{c}_{\alpha,k+q}^\dagger(\tau)\hat{c}_{\alpha,k}(\tau),\end{aligned} \tag{39}$$

where

$$j'^Q_{11}(k) \equiv j^Q_{11}(k), \quad j'^Q_{22}(k) \equiv j^Q_{22}(k),$$
$$j'^Q_{12}(k) = \overline{j'^Q_{21}(k)} \equiv -\frac{a}{\hbar}(t-t')\Delta_k\sin ka. \tag{40}$$

When we use $\widetilde{\hat{J}^Q}$ instead of $\hat{J}^Q$, we obtain the first terms in L_{21} and L_{22} in Eqs. (31). Therefore, this is consistent with the argument by Jonson and Mahan [45] that the heat current operator $\widetilde{\hat{J}^Q}$ leads to SB relations.

In other words, the contributions which violate the SB relations appear in L_{21} and L_{22}, that is, g_k, from the second and third terms in j^Q_{12} in Eq. (17). Furthermore, this g_k is represented by the order parameters of EI, and it contributes not to the electrical conductivity but to the thermal conductivity below the transition temperature.

Although the effect of g_k is small in the present model and does not reproduce the experimental results of Ref. [20] (our model does not directly reflect an electronic and phononic state of Ref. [20], so our result does not explain the experimental results of Ref. [20], which remain as a future problem), this term gives an essentially different contribution to the thermal conductivity, which is beyond the SB relations. It is to be noted that g_k does not appear when one type of interaction is considered. It has already been pointed out that such terms beyond the SB relations do not appear in the Hubbard model [53], and the same argument can be made in this model by mapping the two bands to the spin direction. Also, when $t = t'$, g_k is zero. In other words, it is essential to consider the two types of interactions and the imbalance of transfer integrals in order to obtain a heat current beyond the SB relations.

Finally, we discuss the relationship between the additional contribution to the thermal conductivity and the heat current of excitions. As mentioned in the Introduction, the thermal transport due to excitons is expected to show drastic features, because excitons do not have electronic charges, but have energies contributing to the heat current. The heat current due to excitons is not included in previous studies [10,49], because they are based on the SB relations. However, we find an additional thermal conductivity which does not satisfy the SB relations. Furthermore, the additional thermal conductivity is related to the order parameters of EI. Therefore, it is suggested that the contribution from the heat current carried by excitons is included in the additional thermal conductivity.

In this paper we do not consider the effect of phonons, but we will comment a little on this. The electron-phonon interaction can also lead to a heat current that violates the SB relations, as shown by Jonson and Mahan [45]. However, we think that there is a large difference between the additional contributions due to the electron-phonon interaction and those due to the Coulomb interactions V_b and V_c in our mechanism. The additional contributions due to the electron-phonon interaction exist even above the EI transition temperature, while g_k in our formalism exists only below the EI transition temperature since g_k is characterized by the order parameters of EI. Of course, it is possible that the electron-phonon interaction changes due to the presence of the order parameters of EI, and that the additional contributions can change. However, as far as we consider that the driving force of the EI phase transition is the Coulomb interaction V_b and V_c, the change of the electron-phonon interaction will be subdominant, and the effect of g_k, which is unique to EI phase, will be dominant. Such a theoretical understanding of the exciton's heat current could provide the basis for an experimental determination of the EI state.

VI. CONCLUSION

We study the thermal conductivity in EI using a simple quasi-one-dimensional two-band model with two types of Coulomb interactions between these bands. First, we obtained the heat current operator microscopically and clarified that it cannot be written in the form of an imaginary-time derivative of the electric current operator as Eqs. (17) and (40). In other words, by considering a system with two types of interactions and an imbalance of transfer integrals, an additional heat current operator owing to the excitonic phase transition exists, which is different from previous studies [10,49]. Then, we studied the linear response theory of L_{11}, L_{21}, and L_{22} within a mean-field scheme, and clarified that the above-mentioned additional heat current operator gives contributions in L_{21} and L_{22} which are not expressed in the form of Eqs. (1b) and (1c), or which are beyond the SB relations.

ACKNOWLEDGMENTS

We are grateful to Professor Hidenori Takagi and his group members for fruitful discussions. This work is supported by Grants-in-Aid for Scientific Research from the Japan Society for the Promotion of Science (No. JP20K03802, No. JP18H01162, and No. JP18K03482) and JST-Mirai Program Grant No. JPMJMI19A1, Japan. S.T. is supported by the Japan Society for the Promotion of Science through the Program for Leading Graduate Schools (MERIT).

APPENDIX A: DERIVATIONS OF EQS. (14) AND (16) TOGETHER WITH THE HAMILTONIAN DENSITY

In the preset model [Eq. (4)], the Hamiltonian densities $\hat{h}_i$ and $\hat{h}_{i+\frac{1}{2}}$ are obtained as

$$\begin{aligned}\hat{h}_i =& \left(\frac{t}{2}\hat{c}^\dagger_{1,i}\hat{c}_{1,i+1} + \frac{t}{2}\hat{c}^\dagger_{1,i-1}\hat{c}_{1,i} - t'\hat{c}^\dagger_{2,i-1}\hat{c}_{2,i} + \text{H.c.}\right)\\ &+ (-\epsilon-\mu)\hat{n}_{1,i} + \frac{1}{2}(\epsilon-\mu)(\hat{n}_{2,i}+\hat{n}_{2,i-1})\\ &+ V_b\hat{n}_{1,i}\hat{n}_{2,i} + V_c\hat{n}_{1,i}\hat{n}_{2,i-1}\\ &+ \sum_j\bigg\{V_{\text{imp}}(x_{1,i}-X_j)\hat{n}_{1,i} + V_{\text{imp}}(x_{2,i}-X_j)\frac{\hat{n}_{2,i}}{2}\\ &+ V_{\text{imp}}(x_{2,i-1}-X_j)\frac{\hat{n}_{2,i-1}}{2}\bigg\},\end{aligned}\tag{A1}$$

$$\begin{aligned}\hat{h}_{i+\frac{1}{2}} =& \left(t\hat{c}^\dagger_{1,i}\hat{c}_{1,i+1} - \frac{t'}{2}\hat{c}^\dagger_{2,i-1}\hat{c}_{2,i} - \frac{t'}{2}\hat{c}^\dagger_{2,i}\hat{c}_{2,i+1} + \text{H.c.}\right)\\ &+ \frac{1}{2}(-\epsilon-\mu)(\hat{n}_{1,i+1}+\hat{n}_{1,i}) + (\epsilon-\mu)\hat{n}_{2,i}\\ &+ V_b\hat{n}_{1,i}\hat{n}_{2,i} + V_c\hat{n}_{1,i+1}\hat{n}_{2,i}\\ &+ \sum_j\bigg\{V_{\text{imp}}(x_{1,i+1}-X_j)\frac{\hat{n}_{1,i+1}}{2}\\ &+ V_{\text{imp}}(x_{1,i}-X_j)\frac{\hat{n}_{1,i}}{2} + V_{\text{imp}}(x_{2,i}-X_j)\hat{n}_{2,i}\bigg\}.\end{aligned}\tag{A2}$$

Figure 6 shows the schematic picture of the Hamiltonian density. Using Eqs. (13), (A1), and (A2), the electric and the heat current density operators are expressed as

$$\begin{aligned}\frac{ie}{\hbar}\left[\frac{\hat{n}_{1,i}+\hat{n}_{2,i}}{a},\mathscr{H}\right] &= \frac{2}{a}(\hat{j}_{i+\frac{1}{4}} - \hat{j}_{i-\frac{1}{4}}),\\ \frac{ie}{\hbar}\left[\frac{\hat{n}_{1,i+1}+\hat{n}_{2,i}}{a},\mathscr{H}\right] &= \frac{2}{a}(\hat{j}_{i+\frac{3}{4}} - \hat{j}_{i+\frac{1}{4}}),\\ \frac{i}{\hbar}\left[\frac{\hat{h}_i}{a},\mathscr{H}\right] &= \frac{2}{a}(\hat{j}^Q_{i+\frac{1}{4}} - \hat{j}^Q_{i-\frac{1}{4}}),\\ \frac{i}{\hbar}\left[\frac{\hat{h}_{i+\frac{1}{2}}}{a},\mathscr{H}\right] &= \frac{2}{a}(\hat{j}^Q_{i+\frac{3}{4}} - \hat{j}^Q_{i+\frac{1}{4}}).\end{aligned}\tag{A3}$$

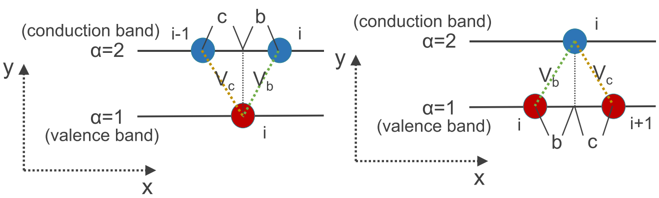

(a) $\hat{h}_i$ (b) $\hat{h}_{i+\frac{1}{2}}$

FIG. 6. Schematic picture of the local (a) ith site, and (b) $(i+1/2)$th site. For the local ith site [$(i+1/2)$th site], we consider hopping in both directions from the ith site in band 1 (band 2), and hopping between the $(i-1)$th site and the ith site in band 2 [between the ith site and the $(i+1)$th site in band 1].

Then, the total electric current and the total heat current operators become

$$\hat{J} = \frac{a}{2}\sum_i \left(\hat{j}_{i+\frac{1}{4}} + \hat{j}_{i+\frac{3}{4}}\right), \quad \hat{J}^Q = \frac{a}{2}\sum_i \left(\hat{j}^Q_{i+\frac{1}{4}} + \hat{j}^Q_{i+\frac{3}{4}}\right) \quad \text{(A4)}$$

As a result, we obtain Eqs. (14) and (16).

APPENDIX B: DISCUSSION ON THE DERIVATION OF HEAT CURRENT OPERATOR

The electric and heat current operators should be uniquely determined once the Hamiltonian is determined, and it should be determined independently of the mean-field approximation. Therefore, the current operators should not be calculated using the mean-field Hamiltonian of Eq. (6), but should be calculated using the original Hamiltonian of Eq. (4) before the mean-field approximation is applied to the heat current operator.

In fact, the electric and heat current operators calculated using the mean-field Hamiltonian (6), $\hat{J}'_{\rm MF}$ and $\hat{J}'^Q_{\rm MF}$, are

$$\hat{J}'_{\rm MF} = \sum_{k,\alpha,\alpha'} j_{\alpha\alpha'}(k)\hat{c}^\dagger_{\alpha,k}\,\hat{c}_{\alpha',k}, \quad \text{(B1)}$$

with

$$j_{11}(k) \equiv j_1(k), \quad j_{22}(k) \equiv j_2(k),$$
$$j_{12}(k) = \overline{j_{21}(k)} \equiv \frac{iea}{2\hbar}(\Delta_b e^{ikb} - \Delta_c e^{-ikc}), \quad \text{(B2)}$$

and

$$\hat{J}'^Q_{\rm MF} = \sum_{k,\alpha,\alpha'} j^Q_{{\rm MF}\alpha\alpha'}(k)\hat{c}^\dagger_{\alpha,k}\,\hat{c}_{\alpha',k} + \sum_{k,q,\alpha,\alpha'} j^Q_{{\rm imp}\alpha\alpha'}(k,q)\hat{c}^\dagger_{\alpha,k+q}\,\hat{c}_{\alpha',k}, \quad \text{(B3)}$$

with

$$j^Q_{\rm MF11}(k) \equiv j^Q_{11}(k) - \frac{a}{\hbar}\Delta_b\,\Delta_c \sin ka,$$
$$j^Q_{\rm MF22}(k) \equiv j^Q_{22}(k) - \frac{a}{\hbar}\Delta_b\,\Delta_c \sin ka,$$
$$j^Q_{\rm MF12}(k) = \overline{j^Q_{\rm MF21}(k)} \equiv -\frac{a}{\hbar}(t-t')\Delta_k \sin ka + \frac{ia}{2\hbar}(\Delta_b e^{ikb} - \Delta_c e^{-ikc})\{(t-t')\cos ka - \mu\},$$
$$j^Q_{\rm imp11}(k) \equiv j^Q_{\rm imp1}(k), \quad j^Q_{\rm imp22}(k,q) \equiv j^Q_{\rm imp2}(k),$$
$$j^Q_{\rm imp12}(k,q) = \overline{j^Q_{\rm imp21}(k)} \equiv \frac{1}{2}\Delta_b\,e^{ikb}(1+e^{iqb}) - \frac{1}{2}\Delta_c\,e^{-ikc}(1+e^{-iqc}). \quad \text{(B4)}$$

These expressions are different from Eq. (17). Furthermore, if we use these operators $\hat{J'_{\rm MF}}$ and $\hat{J'^Q_{\rm MF}}$, we obtain various additional terms compared with Eq. (31).

As this, it is necessary to pay attention to the order of the calculation of the heat current operator and the application of the mean-field approximation.

APPENDIX C: DERIVATIONS OF EQS. (31)

When we define $\Phi^{\alpha\beta}_{\gamma\delta}(k,\omega)$ as an analytic continuation $(i\omega_\lambda \to \hbar\omega + i\delta)$ to $\sum_n \mathscr{G}_{\alpha\beta}(k,i\epsilon_n)\mathscr{G}_{\gamma\delta}(k,i\epsilon_n - i\omega_\lambda)$, the product of the Green's function, we can calculate Eq. (28) by calculating

$$\sigma^{\alpha\beta}_{\gamma\delta}(k) \equiv \left.\frac{\Phi^{\alpha\beta}_{\gamma\delta}(k,\omega) - \Phi^{\alpha\beta}_{\gamma\delta}(k,\omega=0)}{i\omega}\right|_{\omega\to 0}. \quad \text{(C1)}$$

Here, we calculate $\sigma^{++}_{++}(k)$ as an example. Using the Green's function in Eq. (21) and replacing the sum of the Matsubara frequencies with the complex integral, we obtain

$$\sum_n \mathscr{G}_{++}(k,i\epsilon_n - i\omega_\lambda)\mathscr{G}_{++}(k,i\epsilon_n)$$
$$= -\frac{1}{2\pi i k_B T}\int_{-\infty}^{\infty} dx\Bigg[f(x+i\omega_\lambda)\Bigg\{\frac{x-E_{k-}+i\Gamma_2}{(x-E_{k+}+i\Gamma_1)(x-E_{k-}+i\Gamma_2)+\Gamma_3^2}\frac{x+i\omega_\lambda-E_{k-}+i\Gamma_2}{(x+i\omega_\lambda-E_{k+}+i\Gamma_1)(x+i\omega_\lambda-E_{k-}+i\Gamma_2)+\Gamma_3^2}$$
$$-\frac{x-E_{k-}-i\Gamma_2}{(x-E_{k+}-i\Gamma_1)(x-E_{k-}-i\Gamma_2)+\Gamma_3^2}\frac{x+i\omega_\lambda-E_{k-}+i\Gamma_2}{(x+i\omega_\lambda-E_{k+}+i\Gamma_1)(x+i\omega_\lambda-E_{k-}+i\Gamma_2)+\Gamma_3^2}\Bigg\}$$
$$+f(x)\Bigg\{\frac{x-i\omega_\lambda-E_{k-}-i\Gamma_2}{(x-i\omega_\lambda-E_{k+}-i\Gamma_1)(x-i\omega_\lambda-E_{k-}-i\Gamma_2)+\Gamma_3^2}\frac{x-E_{k-}+i\Gamma_2}{(x-E_{k+}+i\Gamma_1)(x-E_{k-}+i\Gamma_2)+\Gamma_3^2}$$

$$-\frac{x-i\omega_\lambda-E_{k-}-i\Gamma_2}{(x-i\omega_\lambda-E_{k+}-i\Gamma_1)(x-i\omega_\lambda-E_{k-}-i\Gamma_2)+\Gamma_3^2}\frac{x-E_{k-}-i\Gamma_2}{(x-E_{k+}-i\Gamma_1)(x-E_{k-}-i\Gamma_2)+\Gamma_3^2}\Big\}\Big]$$
$$=\frac{2}{\pi k_BT}\int_{-\infty}^{\infty}dx\,f(x)\Big[\frac{\{\Gamma_1(x-E_{k-})^2+\Gamma_1\Gamma_2^2-\Gamma_2\Gamma_3^2\}}{\{(x-E_{k+}+i\Gamma_1)(x-E_{k-}+i\Gamma_2)+\Gamma_3^2\}\{(x-E_{k+}-i\Gamma_1)(x-E_{k-}-i\Gamma_2)+\Gamma_3^2\}}$$
$$\times\frac{(x-E_{k+})\{(x-E_{k-})^2-(i\omega_\lambda+i\Gamma_2)^2\}+\Gamma_3^2(x-E_{k-})}{\{(x+i\omega_\lambda-E_{k+}+i\Gamma_1)(x+i\omega_\lambda-E_{k-}+i\Gamma_2)+\Gamma_3^2\}\{(x-i\omega_\lambda-E_{k+}-i\Gamma_1)(x-i\omega_\lambda-E_{k-}-i\Gamma_2)+\Gamma_3^2\}}\Big]. \tag{C2}$$

By performing an analytic continuation ($i\omega_\lambda\to\hbar\omega+i\delta$), we obtain

$$\sigma_{++}^{++}(k)=\frac{4\hbar}{\pi k_BT}\int_{-\infty}^{\infty}dx\,f(x)\frac{\begin{array}{c}\{\Gamma_1^2(x-E_{k+})(x-E_{k-})^6-\Gamma_1\Gamma_2\Gamma_3^2(x-E_{k+})^2(x-E_{k-})^3\\+(3\Gamma_1^2\Gamma_2^2-2\Gamma_1\Gamma_2\Gamma_3^2-\Gamma_1^2\Gamma_3^2)(x-E_{k+})(x-E_{k-})^4+\Gamma_1^2\Gamma_3^2(x-E_{k-})^5\}\end{array}}{\{(x-E_{k+}+i\Gamma_1)(x-E_{k-}+i\Gamma_2)+\Gamma_3^2\}^3\{(x-E_{k+}-i\Gamma_1)(x-E_{k-}-i\Gamma_2)+\Gamma_3^2\}^3}. \tag{C3}$$

And for the denominator of the integrand,

$$\{(x-E_{k+}+i\Gamma_1)(x-E_{k-}+i\Gamma_2)+\Gamma_3^2\}\{(x-E_{k+}-i\Gamma_1)(x-E_{k-}-i\Gamma_2)+\Gamma_3^2\}=\{(x-E_1)^2+\delta_1^2\}\{(x-E_2)^2+\delta_2^2\} \tag{C4}$$

holds, where $E_1=E_{k+}-\frac{\Gamma_3^2}{E_{k+}-E_{k-}}+O(\Gamma^4)$, $E_2=E_{k-}+\frac{\Gamma_3^2}{E_{k+}-E_{k-}}+O(\Gamma^4)$, $\delta_1=\Gamma_1+O(\Gamma^3)$, and $\delta_2=\Gamma_2+O(\Gamma^3)$, where Γ_1, Γ_2, and Γ_3 are written together as Γ. Since we assume that the effect of the impurities is small and Γ is a minute quantity, we can use $\frac{\delta^{2i-1}}{\{(x-a)^2+\delta^2\}^i}\sim\frac{(2i-3)!!}{(2i-2)!!}\pi\,\delta(x-a)$ and $\frac{\delta^{2i-1}(x-a)}{\{(x-a)^2+\delta^2\}^{i+1}}\sim-\frac{(2i-3)!!}{(2i)!!}\pi\,\delta'(x)$ to obtain

$$\begin{aligned}\sigma_{++}^{++}(k)=&\frac{4\hbar}{\pi k_BT}\int_{-\infty}^{\infty}dx\,f(x)\Big[\frac{O(\Gamma^4)}{\{(x-E_1)^2+\delta_1^2\}}+\frac{O(\Gamma^4)}{\{(x-E_2)^2+\delta_2^2\}}+\frac{O(\Gamma^4)}{\{(x-E_1)^2+\delta_1^2\}^2}\\&+\frac{O(\Gamma^6)}{\{(x-E_2)^2+\delta_2^2\}^2}+\frac{O(\Gamma^6)}{\{(x-E_1)^2+\delta_1^2\}^3}+\frac{O(\Gamma^6)}{\{(x-E_2)^2+\delta_2^2\}^3}\\&+\frac{(x-E_1)O(\Gamma^4)}{\{(x-E_1)^2+\delta_1^2\}^2}+\frac{(x-E_2)O(\Gamma^4)}{\{(x-E_2)^2+\delta_2^2\}^2}+\frac{(x-E_1)\{\Gamma_1^2+O(\Gamma^4)\}}{\{(x-E_1)^2+\delta_1^2\}^3}\\&+\frac{(x-E_2)O(\Gamma^6)}{\{(x-E_2)^2+\delta_2^2\}^3}+\frac{O(\Gamma^6)}{\{(x-E_1)^2+\delta_1^2\}\{(x-E_2)^2+\delta_2^2\}}\Big]\\\sim&\frac{4\hbar}{k_BT}\int_{-\infty}^{\infty}dx\,f(x)\Big[\frac{\delta(x-E_1)}{\delta_1}O(\Gamma^4)+\frac{\delta(x-E_2)}{\delta_2}O(\Gamma^4)+\frac{\delta(x-E_1)}{2\delta_1^3}O(\Gamma^4)\\&+\frac{\delta(x-E_2)}{2\delta_2^3}O(\Gamma^6)+\frac{3\delta(x-E_1)}{8\delta_1^5}O(\Gamma^6)+\frac{3\delta(x-E_2)}{8\delta_2^5}O(\Gamma^6)\\&-\frac{\delta'(x-E_1)}{2\delta_1}O(\Gamma^4)-\frac{\delta'(x-E_2)}{2\delta_2}O(\Gamma^4)-\frac{\delta'(x-E_1)}{8\delta_1^3}[\Gamma_1^2+O(\Gamma^4)]\\&-\frac{\delta'(x-E_2)}{8\delta_2^3}O(\Gamma^6)+\frac{\delta(x-E_1)\delta(x-E_2)}{\pi\delta_1\delta_2}O(\Gamma^6)\Big]\\=&\frac{\hbar}{2k_BT\Gamma_1}f'(E_{k+})+O(\Gamma).\end{aligned} \tag{C5}$$

In exactly the same way, we obtain

$$\begin{aligned}&\sigma_{++}^{++}(k)=\frac{\hbar}{2k_BT\Gamma_1}f'(E_{k+})+O(\Gamma),\quad\sigma_{--}^{--}(k)=\frac{\hbar}{2k_BT\Gamma_2}f'(E_{k-})+O(\Gamma),\\&\sigma_{+-}^{+-}(k)=\sigma_{-+}^{+-}(k)=\sigma_{+-}^{-+}(k)=\sigma_{-+}^{-+}(k)=O(\Gamma),\quad\mathrm{Re}[\sigma_{--}^{++}(k)]=\mathrm{Re}[\sigma_{++}^{--}(k)]=O(\Gamma),\\&\mathrm{Re}[\sigma_{+-}^{++}(k)]=\mathrm{Re}[\sigma_{-+}^{++}(k)]=\mathrm{Re}[\sigma_{++}^{+-}(k)]=\mathrm{Re}[\sigma_{++}^{-+}(k)]=O(\Gamma),\\&\mathrm{Re}[\sigma_{+-}^{--}(k)]=\mathrm{Re}[\sigma_{-+}^{--}(k)]=\mathrm{Re}[\sigma_{--}^{+-}(k)]=\mathrm{Re}[\sigma_{--}^{-+}(k)]=O(\Gamma).\end{aligned} \tag{C6}$$

Equation (28) can be calculated by using Eq. (C6), and the result is

$$L_{11}=-\frac{\hbar}{2aN}\sum_k\Big[\frac{f'(E_{k+})}{\Gamma_1}\{|u_{11}|^2j_1(k)+|u_{21}|^2j_2(k)\}^2+\frac{f'(E_{k-})}{\Gamma_2}\{|u_{12}|^2j_1(k)+|u_{22}|^2j_2(k)\}^2\Big]+O(\Gamma). \tag{C7}$$

Here, we defined u_{ij} as the (i,j) component of $\boldsymbol{U}$ in Eq. (9). By calculating Eqs. (29) and (30) in the same way, we obtain

$$L_{21} = -\frac{\hbar}{2aN}\sum_k \Bigg[\frac{f'(E_{k+})}{\Gamma_1}\{|u_{11}|^2 j^Q_{11}(k) + |u_{21}|^2 j^Q_{22}(k) + 2\,\mathrm{Re}[u_{21}\bar{u}_{11}\, j^Q_{12}(k)]\}\{|u_{11}|^2 j_1(k) + |u_{21}|^2 j_2(k)\}$$
$$+\frac{f'(E_{k-})}{\Gamma_2}\{|u_{12}|^2 j^Q_{11}(k) + |u_{22}|^2 j^Q_{22}(k) + 2\,\mathrm{Re}[u_{22}\bar{u}_{12}\, j^Q_{12}(k)]\}\{|u_{12}|^2 j_1(k) + |u_{22}|^2 j_2(k)\}\Bigg] + O(\Gamma), \tag{C8}$$

$$L_{22} = -\frac{\hbar}{2aN}\sum_k \Bigg[\frac{f'(E_{k+})}{\Gamma_1}\{|u_{11}|^2 j^Q_{11}(k) + |u_{21}|^2 j^Q_{22}(k) + 2\,\mathrm{Re}[u_{21}\bar{u}_{11}\, j^Q_{12}(k)]\}^2$$
$$+\frac{f'(E_{k-})}{\Gamma_2}\{|u_{11}|^2 j^Q_{11}(k) + |u_{21}|^2 j^Q_{22}(k) + 2\,\mathrm{Re}[u_{22}\bar{u}_{12}\, j^Q_{12}(k)]\}^2\Bigg] + O(\Gamma). \tag{C9}$$

Using Eqs. (9), (17), and (C1), we can obtain Eq. (31).

[1] N. F. Mott, Philos. Mag. **6**, 287 (1961).
[2] J. M. Blatt, K. W. Böer, and W. Brandt, Phys. Rev. **126**, 1691 (1962).
[3] R. S. Knox, *Theory of Excitons*, Solid State Physics, Suppl. 5 (Academic, New York, 1963).
[4] W. Kohn, Phys. Rev. Lett. **19**, 439 (1967).
[5] D. Jérome, T. M. Rice, and W. Kohn, Phys. Rev. **158**, 462 (1967).
[6] B. I. Halperin and T. M. Rice, Rev. Mod. Phys. **40**, 755 (1968).
[7] J. Zittartz, Phys. Rev. **162**, 752 (1967).
[8] J. Zittartz, Phys. Rev. **164**, 575 (1967).
[9] J. Zittartz, Phys. Rev. **165**, 605 (1968).
[10] J. Zittartz, Phys. Rev. **165**, 612 (1968).
[11] E. W. Fenton, Phys. Rev. **170**, 816 (1967).
[12] B. Bucher, P. Steiner, and P. Wachter, Phys. Rev. Lett. **67**, 2717 (1991).
[13] P. Wachter, Solid State Commun. **118**, 645 (2001).
[14] J. A. Wilson, Solid State Commun. **22**, 551 (1977).
[15] H. Cercellier, C. Monney, F. Clerc, C. Battaglia, L. Despont, M. G. Garnier, H. Beck, P. Aebi, L. Patthey, H. Berger, and L. Forró, Phys. Rev. Lett. **99**, 146403 (2007).
[16] Y. Wakisaka, T. Sudayama, K. Takubo, T. Mizokawa, M. Arita, H. Namatame, M. taniguchi, N. Katayama, M. Nohara, and H. Takagi, Phys. Rev. Lett. **103**, 026402 (2009).
[17] Y. Wakisaka, T. Sudayama, K. Takubo, T. Mizokawa, N. L. Saini, M. Arita, H. Namatame, M. Taniguchi, N. Katayama, M. Nohara, and H. Takagi, J. Supercond. Novel Magn. **25**, 1231 (2012).
[18] K. Seki, Y. Wakisaka, T. Kaneko, T. Toriyama, T. Konishi, T. Sudayama, N. L. Saini, M. Arita, H. Namatame, M. Taniguchi, N. Katayama, M. Nohara, H. Takagi, T. Mizokawa, and Y. Ohta, Phys. Rev. B **90**, 155116 (2014).
[19] J. Neuenschwander and P. Wachter, Phys. Rev. B **41**, 12693 (1990).
[20] P. Wachter, B. Bucher, and J. Malar, Phys. Rev. B **69**, 094502 (2004).
[21] Y. F. Lu, H. Kono, T. I. Larkin, A. W. Rost, T. Takayama, A. V. Boris, B. Keimer, and H. Takagi, Nat. Commun. **8**, 14408 (2017).
[22] T. I. Larkin, A. N. Yaresko, D. Pröpper, K. A. Kikoin, Y. F. Lu, T. Takayama, Y.-L. Mathis, A. W. Rost, H. Takagi, B. Keimer, and A. V. Boris, Phys. Rev. B **95**, 195144 (2017).
[23] T. I. Larkin, R. D. Dawson, M. Höppner, T. Takayama, M. Isobe, Y.-L. Mathis, H. Takagi, B. Keimer, and A. V. Boris, Phys. Rev. B **98**, 125113 (2018).
[24] J. Lee, C.-J. Kang, M. J. Eom, J. S. Kim, B. I. Min, and H. W. Yeom, Phys. Rev. B **99**, 075408 (2019).
[25] J. Yan, R. Xiao, X. Luo, H. Lv, R. Zhang, Y. Sun, P. Tong, W. Lu, W. Song, X. Zhu, and Y. Sun, Inorg. Chem. **58**, 9036 (2019).
[26] S. Y. Kim, Y. Kim, C.-J. Kang, E.-S. An, H. K. Kim, M. J. Eom, M. Lee, C. Park, T.-H. Kim, H. C. Choi, B. I. Min, and J. S. Kim, ACS Nano **10**, 8888 (2016).
[27] K. Fukutani, R. Stania, J. Jung, E. F. Schwier, K. Shimada, C. I. Kwon, J. S. Kim, and H. W. Yeom, Phys. Rev. Lett. **123**, 206401 (2019).
[28] F. X. Bronold and H. Fehske, Phys. Rev. B **74**, 165107 (2006).
[29] K. Seki, R. Eder, and Y. Ohta, Phys. Rev. B **84**, 245106 (2011).
[30] Y. Murakami, D. Golež, M. Eckstein, and P. Werner, Phys. Rev. Lett. **119**, 247601 (2017).
[31] T. Sato, T. Shirakawa, and S. Yunoki, Phys. Rev. B **99**, 075117 (2019).
[32] D. I. Pikulin and T. Hyart, Phys. Rev. Lett. **112**, 176403 (2014).
[33] Z. Jiang, W. Lou, Y. Liu, Y. Li, H. Song, K. Chang, W. Duan, and S. Zhang, Phys. Rev. Lett. **124**, 166401 (2020).
[34] K. Matsubayashi, Meet. Abstr. Phys. Soc. Jpn. **70.1**, 2254 (2015) (in Japanese).
[35] T. Yamada, K. Domon, and Y. Ono, J. Phys. Soc. Jpn. **85**, 053703 (2016).
[36] F. J. Di Salvo, C. H. Chen, R. M. Fleming, J. V. Waszczak, R. G. Dunn, S. A. Sunshine, and J. A. Ibers, J. Less-Common Met. **116**, 51 (1986).
[37] H. Matsuura and M. Ogata, J. Phys. Soc. Jpn. **85**, 093701 (2016).
[38] L. Du, X. Li, W. Lou, G. Sullivan, K. Chang, J. Kono, and R.-R. Du, Nat. Commun. **8**, 1971 (2017).
[39] J. I. A. Li, T. Taniguchi, K. Watanabe, J. Hone, and C. R. Dean, Nat. Phys. **13**, 751 (2017).
[40] X. Liu, K. Watanabe, T. Taniguchi, B. I. Halperin, and P. Kim, Nat. Phys. **13**, 746 (2017).
[41] T. Mizokawa, T. Sudayama, and Y. Wakisaka, J. Phys. Soc. Jpn. **77**, 158 (2008).
[42] T. Kaneko and Y. Ohta, Phys. Rev. B **90**, 245144 (2014).
[43] J. Kuneš, J. Phys.: Condens. Matter **27**, 333201 (2015).

[44] S. Ejima, T. Kaneko, Y. Ohta, and H. Fehske, Phys. Rev. Lett. **112**, 026401 (2014).
[45] M. Jonson and G. D. Mahan, Phys. Rev. B **42**, 9350 (1990).
[46] For example, G. D. Mahan, *Many-Particle Physics* (Plenum, New York, 1990).
[47] M. Ogata and H. Fukuyama, J. Phys. Soc. Jpn. **88**, 074703 (2019).
[48] A. Sommerfeld and H. Bethe, *Elektronentheorie der Metalle*, Handbuch der Physik Vol. 24, Part 2 (Springer, Berlin, 1933).
[49] Y. Kurihara, J. Phys. Soc. Jpn. **33**, 380 (1972).
[50] T. Kaneko, K. Seki, and Y. Ohta, Phys. Rev. B **85**, 165135 (2012).
[51] R. Kubo, J. Phys. Soc. Jpn. **12**, 570 (1957).
[52] J. M. Luttinger, Phys. Rev. **135**, A1505 (1964).
[53] H. Kontani, Phys. Rev. B **67**, 014408 (2003).